Electrochemistry Communications 110 (2020) 106622

Contents lists available at ScienceDirect

Electrochemistry Communications

journal homepage: www.elsevier.com/locate/elecom

New strategy to fabricate a polydopamine functionalized self-supported nanoporous gold film electrode for electrochemical sensing applications

Anandhakumar Sukeri*, Ananthi Arjunan, Mauro Bertotti*

Department of Fundamental Chemistry, Institute of Chemistry, University of São Paulo, Av. Prof. Lineu Prestes, 748, São Paulo, SP, Brazil

ARTICLE INFO

Keywords:
Anodization
Nanoporous gold
Polydopamine
Electrochemical sensors
Hydrogen peroxide
Dopamine

ABSTRACT

In this work, a polydopamine functionalized self-supported nanoporous gold film (PDA@NPGF) was prepared over a Au surface via anodization followed by chemical reduction method using dopamine as a reducing agent for the first time. Field emission scanning electron microscopy (FE-SEM) and energy dispersive X-ray analysis (EDX) were used to characterize the surface morphology and for elemental analysis. The electrocatalytic activity and sensing ability of the PDA@NPGF platform were examined towards hydrogen peroxide (H_2O_2) and dopamine (DA) detection using cyclic voltammetry and amperometry techniques. Cyclic voltammetry results confirm the excellent catalytic activity of the PDA@NPGF electrode for H_2O_2 and DA sensing compared to that of bare Au, and nanoporous gold film (NPGF) electrodes. The electrochemical determination of H_2O_2 and DA at PDA@NPGF was evaluated by amperometry by applying a constant potential of −0.13 V and 0.20 V (*vs.* Ag/AgCl) in the linear range of 1–100 μM, respectively. The detection limit of the developed sensor for H_2O_2 and DA analysis was calculated using the corresponding calibration plots and the values were found to be 0.1 μM and 0.27 μM (S/N = 3), respectively.

1. Introduction

Recently, nanostructured electrodes with large surface area have attracted much attention in electrochemistry because of the great number of adsorption sites for proteins and enzymes immobilization, as well as the electrocatalytic effect owing to the presence of defects and more active sites [1,2]. Therefore, they have been extensively used in catalysis and chemical sensors [3,4], as well as for electrochemical energy conversion [5–9] applications. Such nanostructures are usually prepared through chemical dealloying [10] and/or electrochemical alloying-dealloying [11], electrodeposition via dynamic hydrogen bubble template [12,13], and anodization followed by (i) chemical reduction (using ascorbic acid as reductant) [14] and/or (ii) electrochemical reduction methods [15]. Nanoporous gold (NPG) accomplishes widespread applications and the functionalization of NPG for electrochemical applications is recently emerging. Among many examples, L-Cysteine functionalized NPG film was prepared by self-assembled monolayer based on gold-thiol interaction and used for sensitive and selective detection of Cu (II) ions [16], and a Prussian blue modified NPGF was used for H_2O_2 detection [17].

Polydopamine (PDA), a mussel-inspired polymer, is mostly used in surface chemistry due to the adhesive nature in all materials and is usually prepared by self-polymerization of dopamine in aqueous tris (hydroxymethylaminomethane) buffer solution [18]. PDA films can also be prepared by electro-polymerization of dopamine by cyclic voltammetry [19,20]. The mechanism of PDA formation is still unclear, but the redox property has been largely recognized owing to the presence of catechol/o-quinone moieties, justifying its use for various electrochemical applications [21]. For instance, the literature reports a ferrocene-functionalized polydopamine redox matrix for H_2O_2 oxidation [22], a gold nanoparticle self-assembled on sulfide functionalized polydopamine for nitric oxide oxidation [23], a reduced graphene-oxide@polydopamine composite for fabrication of a chlorpromazine sensor [24], gold nanoparticles-polydopamine-graphene quantum dots nanocomposite for non-enzymatic H_2O_2 detection [25], and biomimetic polydopamine-gold nanocomposite for triglyceride detection [26]. Hitherto, to the best of our knowledge, NPG functionalized with polydopamine was not reported so far. Hence, in this work we present for the first time a simple and reproducible route to fabricate a polydopamine functionalized nanoporous gold film via an anodization followed by chemical reduction method using dopamine as reductant. The electrocatalytic activity of the PDA@NPGF electrode and its ability for sensitive detection were explored using hydrogen peroxide and dopamine as model analytes.

* Corresponding authors.
E-mail addresses: anand@iq.usp.br (A. Sukeri), ananthiarjunan@gmail.com (A. Arjunan), mbertott@iq.usp.br (M. Bertotti).

https://doi.org/10.1016/j.elecom.2019.106622
Received 30 October 2019; Received in revised form 27 November 2019; Accepted 28 November 2019
Available online 03 December 2019

2. Materials and methods

2.1. Chemicals and apparatus

Dopamine hydrochloride (DA), ascorbic acid (AA), hydrogen peroxide (H_2O_2), phosphate buffer saline tablets (to prepare 0.01 M PBS solution of pH 7) and sulfuric acid (H_2SO_4) were acquired from Sigma Aldrich and Merck, respectively. The dissolved oxygen existing in the electrolytic solution was removed by bubbling high pure argon gas (acquired from Oxilumen, Brazil) for 20 min. Milli-Q-water (18.0 MΩ cm resistivity) was used to prepare all the required solutions.

Electrochemical measurements were carried out using a PalmSens portable potentiostat with PSTrace 5.4 version software. Gold (3.0 mm diameter), platinum wire, and Ag/AgCl (saturated KCl) served as working, counter and reference electrodes, respectively. All the potential values are reported versus Ag/AgCl (saturated KCl) reference electrode, unless otherwise stated in this work. Elemental analysis and microscopic images were taken from a field-emission scanning electron microscopy (JOEL JSM-7401F with 30 kV acceleration voltage) instrument.

2.2. Fabrication of the PDA@NPGF electrode

Before anodization, the Au electrode was well-polished with 0.05 μm alumina powder until a reproducible Au response in 0.5 M H_2SO_4 solution was attained. A polydopamine functionalized self-supported nanoporous gold film (hereafter denoted as PDA@NPGF) was fabricated through an anodization followed by chemical reduction method using DA as a reducing agent. Initially, Au oxides (orange-yellow color) were formed over the Au surface by anodization (at 2.0 V for 15 min) in 0.5 M H_2SO_4 solution. The anodized Au electrode was immersed in 0.1 M DA solution for the instantaneous chemical reduction of Au oxides to NPG and oxidation of DA to PDA, leading to the formation of a PDA@NPGF (greenish-black color) on the Au surface (Scheme 1). For comparison, NPG films have been prepared in similar experimental conditions: (i) anodization followed by chemical reduction (A-CR) using ascorbic acid as reductant [14] and (ii) anodization followed by electrochemical reduction (A-ECR) methods (absence of reducing agent) [15].

3. Results and discussion

3.1. Electrochemical and microscopic characterization of PDA@NPGF

Cyclic voltammograms recorded at bare Au, NPGF, and PDA@NPGF electrodes in 0.5 M H_2SO_4 solution are shown in Fig. 1A. The well-characteristic Au oxide formation peak and the corresponding reduction responses can be clearly seen for all these electrodes. However, the voltammogram recorded with the PDA@NPGF electrode showed higher Au oxide formation/reduction currents compared to that of bare Au and NPGF electrodes. The electrochemical surface area (ECSA, calculated using the corresponding Au oxide reduction peak at around 0.9 V by charge-integration method considering a monolayer charge of 390 μC cm^{-2}) and the roughness factor (RF) were determined [15] and the values were found to be 0.3255 cm^2 and 4.61 for bare Au, 1.8370 cm^2 and 26.0 for NPGF, and 3.3205 cm^2 and 47.0 for PDA@NPGF electrodes. Additionally, both parameters (ECSA and RF) were also calculated for NPGF prepared using AA (figure not shown) and the values were determined as 1.444 cm^2 and 20.44. These results clearly confirm that larger ECSA and RF values were obtained for PDA@NPGF compared to other electrodes.

The PDA functionalization of the NPGF surface was established by the presence of a well-defined surface-controlled redox response corresponding to DA oxidation/reduction process at the formal potential of 0.27 V in 0.01 M PBS solution (Fig. 1B, inset), which was further confirmed by the linearity obtained in the oxidation current *vs* scan rate plot (Fig. 1B).

Surface morphology of NPGF (prepared by A-ECR method) and PDA@NPGF was assessed by FE-SEM. A well-known three-dimensional nanoporous network structure with pore sizes around 30–50 nm was observed for NPGF (Fig. 2A), and such structures are completely sheltered with PDA functionalization, as shown in Fig. 2B. For comparison, an NPGF was also prepared using ascorbic acid as reductant under identical conditions and a similar structure as the one presented in Fig. 2A was obtained, with pore sizes in the range 30–60 nm. Additionally, the presence of the elements C, N, O, and Au existing in the PDA@NPGF was confirmed by EDX analysis and, for comparison, the NPGF was also analyzed and only Au atoms were noticed. Hence, the presence of a PDA redox moiety within an NPGF with a high surface area fabricated by this simple approach can be more beneficial for various electrochemical applications.

3.2. Electrocatalytic H_2O_2 reduction at PDA@NPGF

In a recent work we have demonstrated that thicker NPG films present higher energy crystal planes and structural defects that cannot be found at bare gold surfaces [27]. At such platform, the anodic oxidation of ascorbate takes place at less positive potential values, hence it is likely that the electron transfer process is facilitated owing to the presence of such low coordinated gold atoms. A similar result was noticed for H_2O_2, i.e., the peak potential was shifted to less negative values by using the NPGF electrode in comparison to the bare electrode (Fig. 3A, curves a and b). Such effect is even more pronounced for the PDA@NPGF electrode, where enhanced reduction current (approx. 2-fold) was achieved compared to the other two electrodes (Fig. 3A, curve c). Moreover, the peak potential for the H_2O_2 electroreduction at the PDA@NPGF electrode (−0.13 V) was shifted towards less negative potential values compared to that of bare Au (−0.65 V) and NPGF (−0.35 V), respectively, probably because PDA (present in the NPGF) is also a good redox mediator and hence it can contribute to the electrocatalytic effect. It should be pointed out that the H_2O_2 reduction current did not increase proportionally with the electrochemical active surface area. This can be reasoned as the H_2O_2 reduction takes place at the outer porous surface of the PDA@NPGF and hence the electroactive area of the inner porous surface is not significantly involved in the overall H_2O_2 reduction reaction.

We have recently developed H_2O_2 sensors based on NPG fabricated by A-ECR and dynamic hydrogen bubble template methods, and the peak

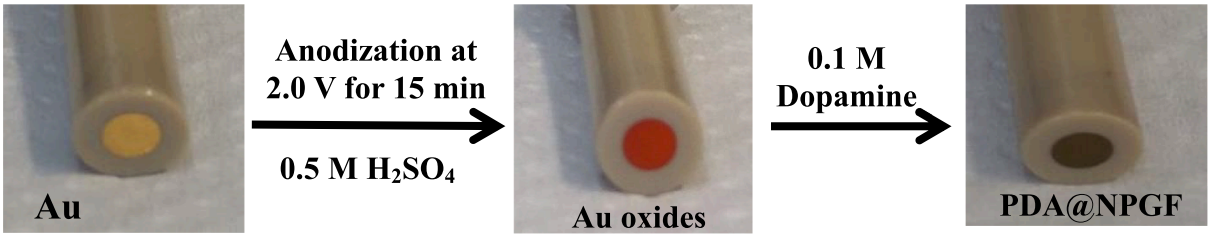

Scheme 1. Fabrication of PDA@NPGF via anodization followed by chemical reduction method.

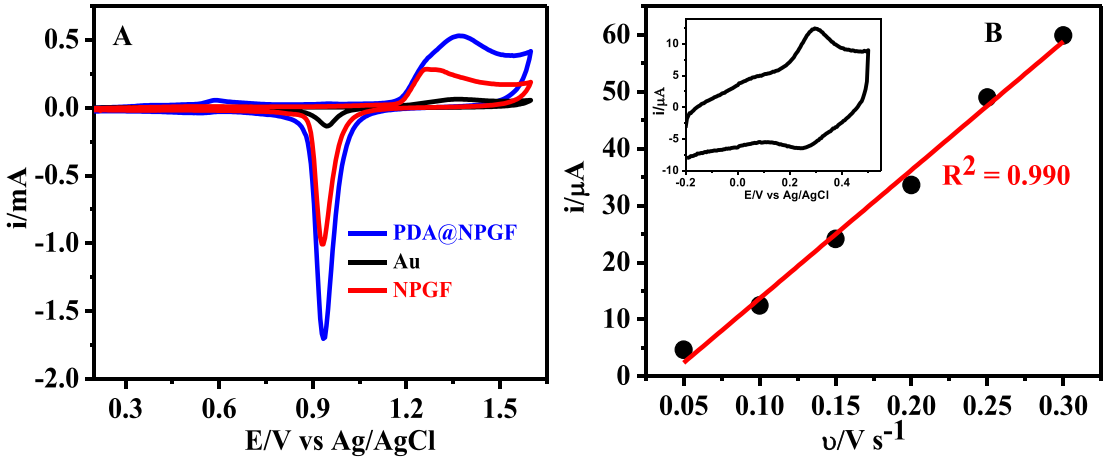

Fig. 1. CV responses of bare Au, NPGF, and PDA@NPGF electrodes in 0.5 M H_2SO_4 solution at the scan rate of 0.1 V s^{-1} (A); CV behavior of PDA@NPGF electrode in 0.01 M PBS solution (inset) and the corresponding current *vs*. scan rate plot (B).

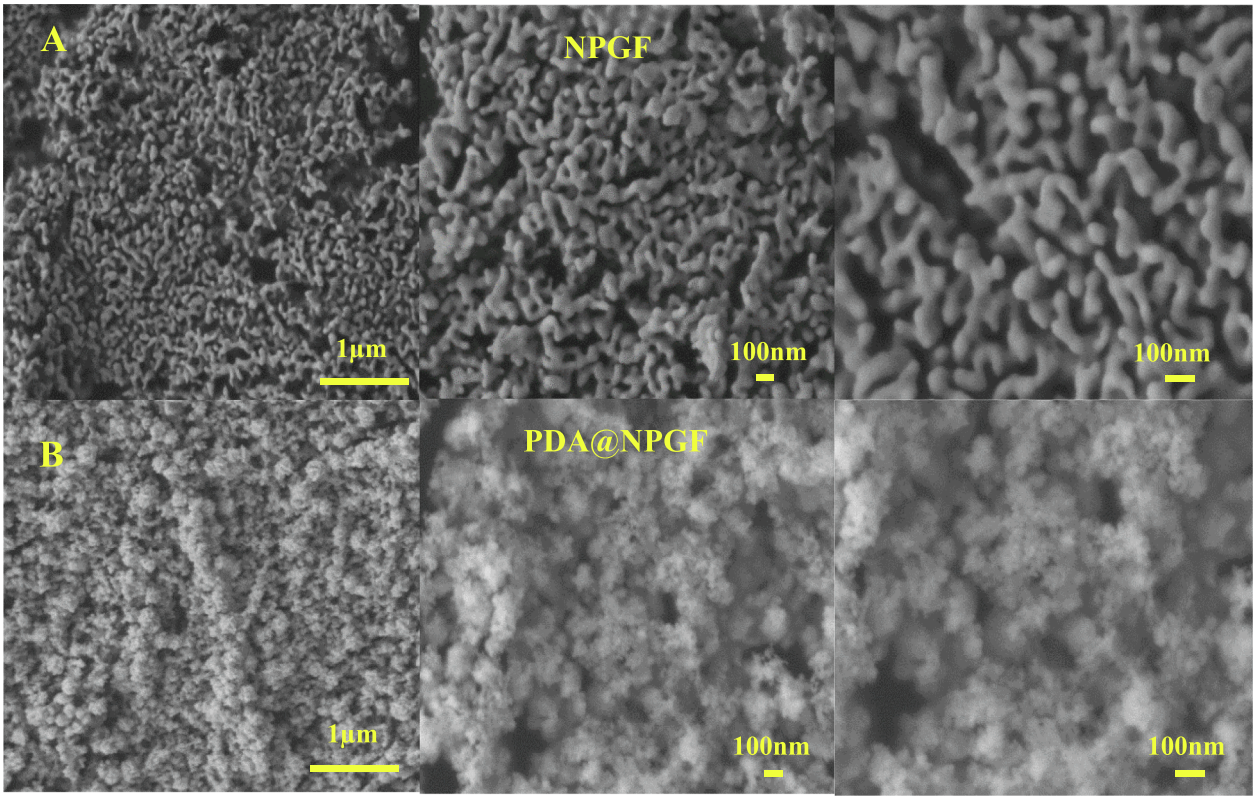

Fig. 2. FE-SEM images of NPGF (A) and PDA@NPGF (B) at different magnifications.

potential for the H_2O_2 reduction process was found to be −0.2 V and −0.1 V, respectively [28,29]. NPG electrodes prepared by a well-known dealloying method using Au-Sn or Au-Ag alloys showed H_2O_2 reduction potentials at −0.42 V and −0.35 V, respectively [30,31], and such values are 0.29 V and 0.22 V more negative compared to that obtained with the PDA@NPGF electrode. For comparison, we have also prepared NPGF by A-CR method using ascorbic acid as reductant at the same experimental conditions and the H_2O_2 reduction peak was noticed at −0.43 V which is around 0.30 V more negative than that of PDA@NPGF.

In order to shed light on the mechanism regarding the electrochemical reduction of H_2O_2 at the PDA@NPGF electrode, scan rate dependent CVs were recorded from 0.01 to 0.1 V s^{-1}. Fig. 3B shows the current *vs* square root of the scan rate plot and the linear dependence confirms the electrochemical process is diffusion-controlled. Hence, the above results suggest that PDA@NPGF can be a suitable platform for electrocatalytic H_2O_2 reduction at less negative potentials for the development of non-enzymatic H_2O_2 sensors.

The analytical performance of the PDA@NPGF towards H_2O_2 reduction was assessed by applying a constant potential of −0.13 V during successive additions of H_2O_2 in the linear range of 1–100 μM (Fig. 3C). As it can be seen, a proportional current increment was observed with H_2O_2 additions. From the calibration plot (Fig. 3D), a sensitivity of 2.53 μA μM^{-1} cm^{-2} and a detection limit of 0.1 μM (S/N = 3) were calculated. The obtained LOD is much lower compared to the values reported for other nanoporous gold based H_2O_2 sensors, i.e., 3.7 μM [28], 3.0 μM [29], 10 μM [30] and 3.26 μM [31], revealing the excellent performance of the developed PDA@NPGF electrode towards H_2O_2 detection.

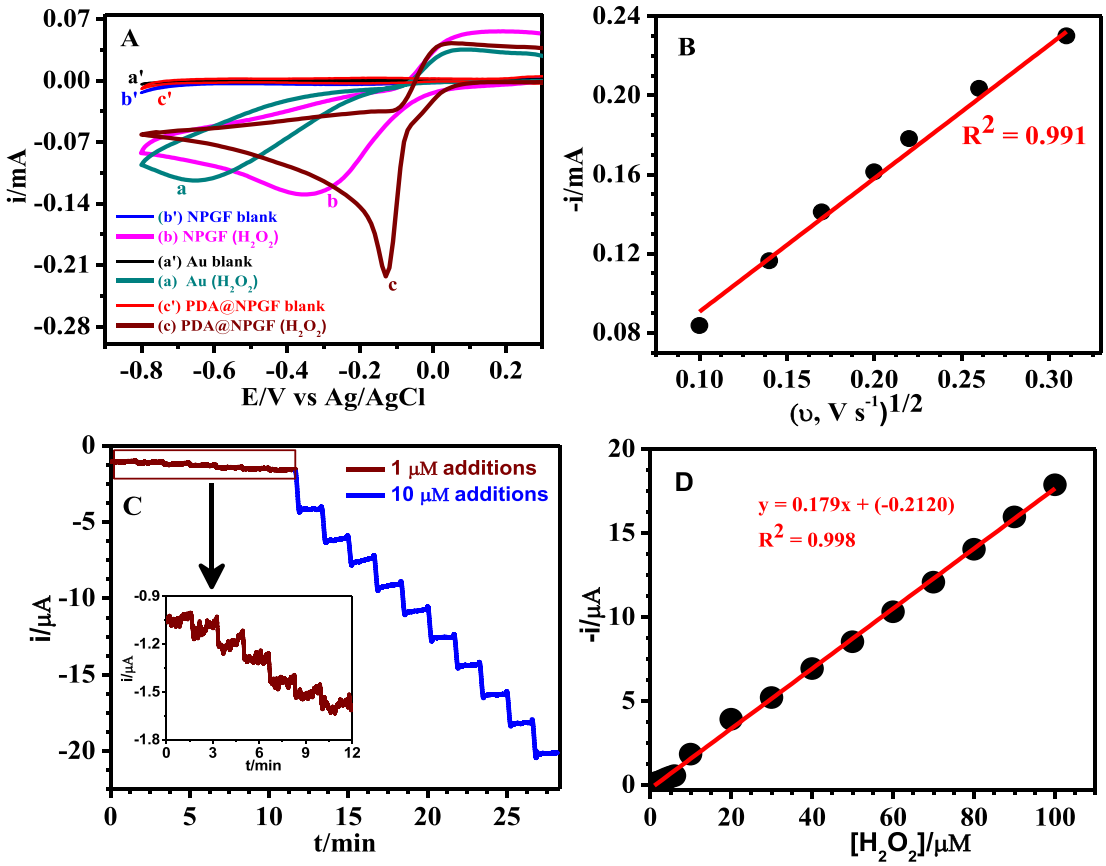

Fig. 3. (A) CVs of H_2O_2 reduction (5.0 mM) at (a) bare Au; (b) NPGF; and (c) PDA@NPGF electrodes in 0.01 M PBS solution (a', b'& c' are the corresponding backgrounds), scan rate 0.1 V s^{-1}; (B) i *vs.* $\upsilon^{1/2}$ plot for the H_2O_2 reduction (5.0 mM) at the PDA@NPGF electrode; (C) amperometric i-t responses for successive addition of [H_2O_2] at a constant potential of −0.13 V using the PDA@NPGF electrode; (D) corresponding calibration plot.

3.3. Sensitive determination of dopamine at PDA@NPGF

After the successful assessment of the PDA@NPGF electrode for H_2O_2 reduction, the sensor was employed for electrochemical oxidation reactions and DA was chosen as a model analyte. The voltammograms recorded in absence (a', b' & c') and presence of DA (1.0 mM) in PBS solution at bare Au (a), NPGF (b), and PDA@NPGF (c) electrodes were shown in Fig. 4A. No faradaic response was observed for bare Au and NPGF electrodes in absence of DA (a' & b'), whereas a characteristic redox peak was noticed for the PDA@NPGF electrode (c'), which is attributable to the presence of PDA in the NPGF structures. However, distinct redox responses were observed at the formal potential of around 0.15 V for all electrodes in the presence of DA [32]. As already observed for H_2O_2 reduction, a higher peak current value for DA oxidation was obtained using the NPGF electrode because the increased electroactive surface area. Such oxidation current was enhanced around 3.5 and 2-fold at the PDA@NPGF electrode compared to bare Au and NPGF electrodes, respectively. Thus, the obtained results clearly indicate both NPGF (high surface area) and PDA (redox mediator) can be responsible for the overall current increment. For comparison, NPGF can also be prepared using ascorbic acid under identical condition and a similar response to the one obtained with the NPGF prepared by the A-ECR method was obtained for DA oxidation. However, the DA oxidation current was 2-fold enhanced by using the PDA@NPGF electrode.

In order to examine the electrochemical process of DA at the PDA@NPGF electrode, cyclic voltammograms were recorded at different scan rates (0.01–0.20 V s^{-1}). The resulting current *vs* scan rate plot (Fig. 4B) shows linear behavior for both DA oxidation and reduction with correlation coefficients of 0.997 and 0.999, respectively, which indicates the existence of a surface-controlled process. Hence, in order to utilize the mutual advantages of PDA and NPGF, one can use the PDA@NPGF as a sensing platform for sensitive determination of DA. Accordingly, Fig. 4C shows amperometric responses regarding DA oxidation using the PDA@NPGF electrode at an applied potential of 0.20 V. A linear increment of current was observed with consecutive additions of DA in the concentration ranges from 1 to 100 μM. The limit of detection and sensitivity were calculated from the slope of the corresponding calibration plot (Fig. 4D) and the obtained values were 0.27 μM and 1.0 μA μM^{-1} cm^{-2}, respectively. The calculated LOD is comparable to values reported for other DA sensors based on nanoporous gold: 1.5 μM [33] 1.0 μM [34], 0.2 μM [35], 0.1 μM [36], and 0.1 μM [37].

4. Conclusions

We have successfully fabricated a PDA@NPGF electrode and demonstrated the dual advantages (such as high surface area and redox moiety) of the developed sensor towards H_2O_2 and DA detection. The observed electrochemical results clearly suggest the remarkable electrocatalytic activity for H_2O_2 reduction and improved sensing ability of the proposed electrode for both analytes. Henceforth, the PDA@NPGF can be an attractive material for several potential applications in the area of electrochemical sensors.

CRediT authorship contribution statement

Anandhakumar Sukeri: Conceptualization, Methodology, Investigation, Writing - original draft. **Ananthi Arjunan:** Investigation, Validation. **Mauro Bertotti:** Supervision.

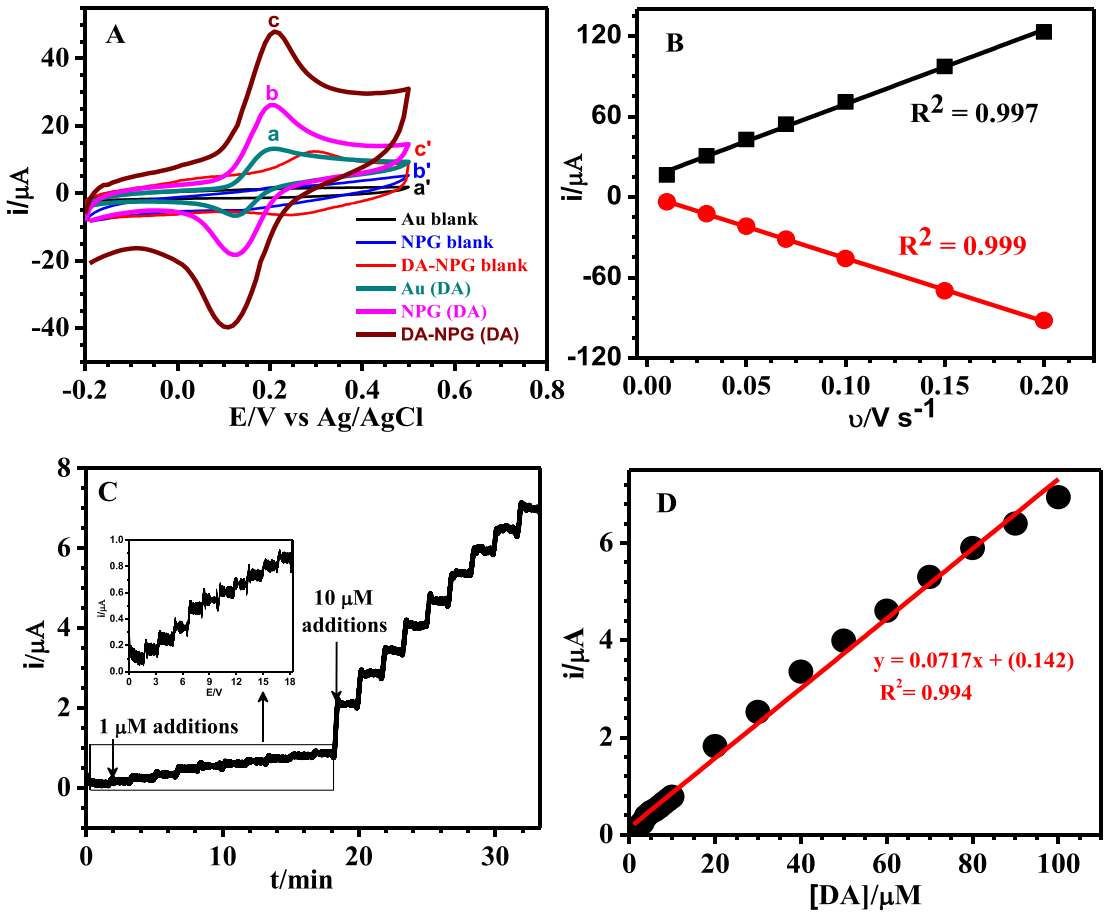

Fig. 4. (A) CVs of DA oxidation (1.0 mM) at (a) bare Au; (b) NPGF; and (c) PDA@NPGF electrodes in 0.01 M PBS solution (a', b'& c' are the corresponding backgrounds), scan rate 0.1 V s^{-1}; (B) i *vs.* υ plot; (C) amperometric i-t responses for consecutive additions of DA at applied potential of 0.20 V; (D) corresponding calibration plot.

Declaration of Competing Interest

The authors declare that they have no known competing financial interests or personal relationships that could have appeared to influence the work reported in this paper.

Acknowledgements

SAK (Grant No. 150177/2018-6) and AA (Grant No. 155422/2018-9) thank National Council for Scientific and Technological Development (CNPq), Brazil for the award of postdoctoral fellowships. All the authors gratefully acknowledge CNPq and FAPESP (Sao Paulo Research Foundation, Grants 2014/15215-5 and 2018/08782-1) for unceasing financial support. Further, we thank Victor Basile Astuto for assisting to take FE-SEM images.

References

[1] F. Jia, C. Yu, Z. Ai, L. Zhang, Fabrication of nanoporous gold film electrodes with ultrahigh surface area and electrochemical activity, Chem. Mater. 19 (2007) 3648–3653, https://doi.org/10.1021/cm070425l.
[2] K.J. Stine, Nanoporous gold and other related materials, Nanomaterials 9 (2019) 1080, https://doi.org/10.3390/nano9081080.
[3] A. Wittstock, J. Biener, M. Bäumer, Nanoporous gold: a new material for catalytic and sensor applications, Phys. Chem. Chem. Phys. 12 (2010) 12919–12930, https://doi.org/10.1039/c0cp00757a.
[4] S.H. Kim, Nanoporous gold: preparation and applications to catalysis and sensors, Curr. Appl. Phys. 18 (2018) 810–818, https://doi.org/10.1016/j.cap.2018.03.021.
[5] L.P. Hernández-Saravia, A. Sukeri, M. Bertotti, Fabrication of nanoporous gold-islands via hydrogen bubble template: an efficient electrocatalyst for oxygen reduction and hydrogen evolution reactions, Int. J. Hydrogen Energy 44 (2019) 15001–15008, https://doi.org/10.1016/j.ijhydene.2019.04.186.
[6] R. Guo, X. Xu, Y. Xia, W. Huang, Z. Li, B. Teng, Insights into electrocatalytic hydrogen evolution reaction in acidic medium at in-situ dispersed Pt atoms on nanoporous gold films, J. Catal. 368 (2018) 379–388, https://doi.org/10.1016/j.jcat.2018.10.026.
[7] A. Sukeri, M. Bertotti, Nanoporous gold surface: an efficient platform for hydrogen evolution reaction at very low overpotential, J. Braz. Chem. Soc. 29 (2018) 226–231, https://doi.org/10.21577/0103-5053.20170132.
[8] X. Xiao, C. Engelbrekt, Z. Li, P. Si, Hydrogen evolution at nanoporous gold/tungsten sulfide composite film and its optimization, Electrochim. Acta 173 (2015) 393–398, https://doi.org/10.1016/j.electacta.2015.05.048.
[9] A. Kiani, S. Hatami, Fabrication of platinum coated nanoporous gold film electrode: a nanostructured ultra low-platinum loading electrocatalyst for hydrogen evolution reaction, Int. J. Hydrogen Energy 35 (2010) 5202–5209, https://doi.org/10.1016/j.ijhydene.2010.03.014.
[10] Y. Ding, Y.-J. Kim, J. Erlebacher, Nanoporous gold leaf: 'ancient technology', Adv. Mater. 16 (2004) 1897–1900, https://doi.org/10.1002/adma.200400792.
[11] K. Rong, L. Huang, H. Zhang, J. Zhai, Y. Fang, S. Dong, Electrochemical fabrication of nanoporous gold electrodes in a deep eutectic solvent for electrochemical detections, Chem. Commun. 54 (2018) 8853–8856, https://doi.org/10.1039/C8CC04454F.
[12] B.J. Plowman, L.A. Jones, S.K. Bhargava, Building with bubbles: the formation of high surface area honeycomb-like films via hydrogen bubble templated electrodeposition, Chem. Commun. 51 (2015) 4331–4346, https://doi.org/10.1039/C4CC06638C.
[13] A. Kumar, J.M. Gonçalves, A. Sukeri, K. Araki, M. Bertotti, Correlating surface growth of nanoporous gold with electrodeposition parameters to optimize amperometric sensing of nitrite, Sensors Actuators, B Chem. 263 (2018) 237–247, https://doi.org/10.1016/j.snb.2018.02.125.
[14] N. Jia, L. Cao, Z. Wang, Platinum-coated gold nanoporous film surface: electrodeposition and enhanced electrocatalytic activity for methanol oxidation, Langmuir 24 (2008) 5932–5936, https://doi.org/10.1021/la800163f.
[15] A. Sukeri, L.P.H. Saravia, M. Bertotti, A facile electrochemical approach to fabricate a nanoporous gold film electrode and its electrocatalytic activity towards dissolved oxygen reduction, Phys. Chem. Chem. Phys. 17 (2015) 28510–28514, https://doi.org/10.1039/C5CP05220C.
[16] J.-F. Huang, I.-W. Sun, Fabrication and surface functionalization of nanoporous gold by electrochemical alloying/dealloying of Au-Zn in an ionic liquid, and the

self-assembly of L-cysteine monolayers, Adv. Funct. Mater. 15 (2005) 989–994, https://doi.org/10.1002/adfm.200400382.
[17] S. Ghaderi, M.A. Mehrgardi, Bioelectrochemistry Prussian blue-modi fi ed nanoporous gold fi lm electrode for amperometric determination of hydrogen peroxide, Bioelectrochemistry 98 (2014) 64–69. doi:10.1016/j.bioelechem.2014.03.007.
[18] J.H. Ryu, P.B. Messersmith, H. Lee, Polydopamine surface chemistry: a decade of discovery, ACS Appl. Mater. Interfaces 10 (2018) 7523–7540, https://doi.org/10.1021/acsami.7b19865.
[19] G. Loget, J.B. Wood, K. Cho, A.R. Halpern, R.M. Corn, Electrodeposition of polydopamine thin films for DNA patterning and microarrays, Anal. Chem. 85 (2013) 9991–9995, https://doi.org/10.1021/ac4022743.
[20] P. Kanyong, S. Rawlinson, J. Davis, Sensors and Actuators B: chemical fabrication and electrochemical characterization of polydopamine redox polymer modified screen-printed carbon electrode for the detection of guanine, Sensors Actuators B. Chem. 233 (2016) 528–534, https://doi.org/10.1016/j.snb.2016.04.099.
[21] J. Liebscher, R. Mrówczyński, H.A. Scheidt, C. Filip, N.D. Hădade, R. Turcu, A. Bende, S. Beck, Structure of polydopamine: a never-ending story? Langmuir 29 (2013) 10539–10548, https://doi.org/10.1021/la4020288.
[22] T.N. Kumar, S. Sivabalan, K.L.N. Phani, Ferrocene-functionalized polydopamine as a novel redox matrix for H 2 O 2 oxidation, J. Mater. Chem. B 2 (2014) 6081–6088, https://doi.org/10.1039/C4TB00823E.
[23] A. Ananthi, K.L. Phani, Self-assembly of gold nanoparticles on sulphide functionalized polydopamine in application to electrocatalytic oxidation of nitric oxide, J. Electroanal. Chem. 764 (2016) 7–14, https://doi.org/10.1016/j.jelechem.2016.01.003.
[24] S. Palanisamy, B. Thirumalraj, S. Chen, Y. Wang, A facile electrochemical preparation of reduced graphene oxide @ polydopamine composite: a novel electrochemical sensing platform for amperometric detection of chlorpromazine, Sci. Rep. 6 (2016) 33599, https://doi.org/10.1038/srep33599.
[25] Y. Zhu, S. Lu, A.G. Manohari, X. Dong, F. Chen, W. Xu, Z. Shi, C. Xu, Polydopamine interconnected graphene quantum dots and gold nanoparticles for enzymeless H_2O_2 detection, J. Electroanal. Chem. 796 (2017) 75–81, https://doi.org/10.1016/j.jelechem.2017.04.017.
[26] W. Zhang, Y. Tang, J. Liu, Y. Ma, L. Jiang, W. Huang, F.W. Huo, D. Tian, An electrochemical sensor for detecting triglyceride based on biomimetic polydopamine and gold nanocomposite, J. Mater. Chem. B 2 (2014) 8490–8495, https://doi.org/10.1039/C4TB01439A.
[27] A. Kumar, J.M. Goncalves, J.S.G. Selva, K. Araki, M. Bertotti, Correlating selective electrocatalysis of dopamine and ascorbic acid electrooxidation at nanoporous gold surfaces with structural-defects, J. Electrochem. Soc. 166 (2019) H704–H711, https://doi.org/10.1149/2.0821914jes.
[28] A. Sukeri, A.S. Lima, M. Bertotti, Development of non-enzymatic and highly selective hydrogen peroxide sensor based on nanoporous gold prepared by a simple unusual electrochemical approach, Microchem. J. 133 (2017) 149–154, https://doi.org/10.1016/j.microc.2017.03.023.
[29] A. Sukeri, M. Bertotti, Electrodeposited honeycomb-like dendritic porous gold surface: an efficient platform for enzyme-free hydrogen peroxide sensor at low overpotential, J. Electroanal. Chem. 805 (2017) 18–23, https://doi.org/10.1016/j.jelechem.2017.10.004.
[30] X. Ke, Z. Li, L. Gan, J. Zhao, G. Cui, W. Kellogg, D. Matera, D. Higgins, G. Wu, Three-dimensional nanoporous Au films as high-efficiency enzyme-free electrochemical sensors, Electrochim. Acta 170 (2015) 337–342, https://doi.org/10.1016/j.electacta.2015.04.144.
[31] F. Meng, X. Yan, J. Liu, J. Gu, Z. Zou, Electrochimica Acta nanoporous gold as non-enzymatic sensor for hydrogen peroxide, Electrochim. Acta 56 (2011) 4657–4662, https://doi.org/10.1016/j.electacta.2011.02.105.
[32] H.S.C. Sáenz, L.P. Hernández-Saravia, J.S.G. Selva, A. Sukeri, P.J. Espinoza-Montero, M. Bertotti, Electrochemical dopamine sensor using a nanoporous gold microelectrode: a proof-of-concept study for the detection of dopamine release by scanning electrochemical microscopy, Microchim. Acta 185 (2018) 367, https://doi.org/10.1007/s00604-018-2898-z.
[33] P.Y. Ge, Y. Du, J.J. Xu, H.Y. Chen, Selective detection of dopamine based on the unique property of gold nanofilm, J. Electroanal. Chem. 633 (2009) 182–186, https://doi.org/10.1016/j.jelechem.2009.05.010.
[34] X. Yi, Y. Wu, G. Tan, P. Yu, L. Zhou, Z. Zhou, et al., Palladium nanoparticles entrapped in a self-supporting nanoporous gold wire as sensitive dopamine biosensor, Sci. Rep. 7 (2017) 7941, https://doi.org/10.1038/s41598-017-07909-y.
[35] J. Hou, C. Xu, D. Zhao, J. Zhou, Facile fabrication of hierarchical nanoporous AuAg alloy and its highly sensitive detection towards dopamine and uric acid, Sensors Actuators, B Chem. 225 (2016) 241–248, https://doi.org/10.1016/j.snb.2015.11.035.
[36] W.A. El-Said, J.H. Lee, B.K. Oh, J.W. Choi, 3-D nanoporous gold thin film for the simultaneous electrochemical determination of dopamine and ascorbic acid, Electrochem. Commun. 12 (2010) 1756–1759, https://doi.org/10.1016/j.elecom.2010.10.015.
[37] A. Kumar, J.S.G. Selva, J.M. Gonçalves, K. Araki, M. Bertotti, Nanoporous gold-based dopamine sensor with sensitivity boosted by interferant ascorbic acid, Electrochim. Acta 322 (2019), https://doi.org/10.1016/j.electacta.2019.134772.